

Effect of Cu and Ge on solute clustering in Al-Mg-Si alloys

Meng Liu^{a,b,*}, John Banhart^{a,b}

^a Helmholtz-Zentrum Berlin, Hahn-Meitner-Platz 1, D-14109 Berlin, Germany

^b Technische Universität Berlin, Hardenbergstr. 36, D-10623 Berlin, Germany

* Corresponding author at: Helmholtz-Zentrum Berlin, Hahn-Meitner-Platz 1, D-14109 Berlin, Germany
Tel.: +49 30 8062 – 43099; fax: +49 30 8062 – 43059; Email address: meng.liu@helmholtz-berlin.de

Abstract

The clustering kinetics after quenching and during natural ageing in pure or Cu/Ge-containing Al-Mg-Si alloys was studied by positron annihilation lifetime spectroscopy and hardness measurements. The evolution of positron lifetime follows qualitatively the same pattern for all the alloys investigated, but also differs in some details: adding Cu to both Al-Mg-Si and Al-Mg-Ge alloys slows down the initial formation of clusters in all alloys. However, in Al-Mg-Si alloys, it promotes their growth in later stages. For Ge-containing Al-Mg-Si alloys with equal Mg contents, Ge notably retards the ageing kinetics compared to Si. Possible reasons of these effects are related to the interactions between vacancies and solutes or solute clusters and to the diffusion kinetics of various solute-vacancy complexes.

Keywords: Al-Mg-Si alloys; Cu addition; Ge addition; Solute clustering; Age hardening; Positron annihilation lifetime spectroscopy

1. Introduction

The detrimental effect of natural ageing (NA) on subsequent artificial ageing (AA) in Al-Mg-Si alloys, i.e. the slower and less pronounced increase of hardness [1], is caused by the formation of solute clusters during room temperature storage after quenching [2]. Various methods have been suggested to suppress this negative effect: the strength response during AA can be considerably improved through prior pre-ageing [3,4], pre-straining [5,6], or the combination of both treatments [7,8]. It was also found that the diffusion of solute atoms mediated by quenched-in vacancies can be controlled by adding small amounts of an alloying element such as Cu [9], which slows down the formation of deleterious solute clusters during NA. The direct visualization of such clusters is quite challenging, on the one hand due to the low solute content of the investigated alloys (giving rise to a low signal-to-noise ratio), on the other due to the

similar electronic configuration of Mg, Al and Si atoms (leading to low elemental contrast). Conventional electron microscopy and even atom probe tomography have failed to follow the rapid formation and evolution of these clusters in early stages of NA. Some information on solute clustering was obtained by using integral methods such as hardness and electrical resistivity measurement, differential scanning calorimetry and positron annihilation lifetime spectroscopy (PALS) [10]. Especially PALS has shown its power in revealing the cluster formation processes immediately after quenching [11] and appears suitable for further studies of the interactions between various solute atoms and vacancies during NA.

In this study, the effect of Cu and Ge atoms on the clustering kinetics of Al-Mg-Si alloys was investigated. Cu addition has been found to reduce the deleterious effect of NA and to help to achieve the desired mechanical properties through producing finer structures during AA [12,13]. However, little is known about how Cu atoms influence the clustering kinetics of Al-Mg-Si alloys during NA. In other studies, the alloying element Si was partially or fully replaced by Ge since the two elements have a similar electron configuration and similar precipitation properties are expected. Although Ge is considerably larger compared to Si in terms of atomic radius, previous studies have shown that the precipitation processes in Al-Mg-Si and Al-Mg-Ge alloys are alike [14]. Therefore, it is of great interest to carry out investigations on Al-Mg-Ge or Al-Mg-Si-Ge alloys. All these effects were investigated by means of PALS and hardness measurements in this study [15].

2. Experiments

2.1 Sample preparation

Two alloys – 4-10 and 4-10Cu – were cast by Hydro Aluminium Bonn. All other alloys were provided by SINTEF, Norway. The chemical compositions as determined by inductively coupled plasma optical emission spectrometry (ICP-OES) show impurity levels below 100 ppm. The measured compositions of all the samples are given in Table 1. They fall into two groups: Al-Mg-Si alloys with and without Cu addition and alloys in which Si has been fully or partially replaced by Ge. In the latter group, some alloys also contain Cu.

Table 1. Composition of the alloys investigated. “-” means <0.01 (all in at.%).

Designation	Mg	Si	Cu	Ge
A2	0.41	0.83	-	-
A2Cu	0.50	0.87	0.12	-
A3	0.57	0.66	-	-
A3Cu	0.65	0.70	0.07	-
A11	0.84	0.40	-	-
A11Cu	0.86	0.45	0.11	-
4-10	0.44	0.97	-	-
4-10Cu	0.41	0.96	0.02	-
G3	0.22	-	-	0.59
G11	0.25	-	-	0.14
G11Cu	0.24	-	0.11	0.13
GS3	0.24	0.31	-	0.20
GS11	0.44	0.18	-	0.04
GS11Cu	0.45	0.18	0.13	0.05

The samples used for PALS and hardness measurement had a size of $(10 \times 10 \times 1) \text{ mm}^3$. All samples were cut from homogenized (24 h at 530 °C) and extruded bars to the required geometry, followed by mechanical grinding and ultrasonic cleaning in alcohol to reduce surface contaminations. Solution heat treatment was carried out for 1 h at 540 °C for the Cu-containing alloys, for 1 h at 600 °C for the Ge-containing alloys. In the furnace, the samples were held in a block of Ni metal acting as a thermal reservoir in an argon atmosphere. During quenching, the samples and the reservoir drop together. Before reaching the surface of the quenching medium (iced water), the reservoir is blocked by a stopper, while the samples are pulled out of the reservoir and are dragged into the quenching medium. Thus, premature cooling during dropping is prevented by the reservoir due to its large heat capacity and a high quenching rate is ensured [16]. After quenching, the PALS samples were immediately cleaned with alcohol, dried, and assembled to the required sandwich geometry consisting of two samples with the positron emitter in between. This handling usually took 1 min to 2 min. The samples for hardness measurement were polished before and after quenching to achieve a mirror surface, which took ~5 min.

2.2 PALS and hardness measurements

The positron lifetime (PLT) can be measured as the time difference between the 1.275 MeV γ emission by a decaying ^{22}Na nucleus, which almost coincides with the positron emission (start signal), and one of the 0.511 MeV annihilation events (stop signal). As an example, the positron lifetime τ equals ~ 0.165 ns in bulk Al, but in the presence of an open-volume defect such as a mono-vacancy the lifetime of a positron trapped here increases to ~ 0.250 ns due to the locally reduced electron density. Moreover, positrons can also annihilate in solute clusters of a certain size formed during NA, with a PLT depending on cluster properties [17,18]. Based on this feature, defect types and concentrations can be determined according to their lifetimes and corresponding intensities.

An analog “fast-fast” coincidence spectrometer was used for the in-situ PALS experiments. The positron source ^{22}Na enclosed in Kapton foil had an activity of ~ 15 μCi . After packing the source with two identical samples situated on both sides into Al foil, such a “sandwich” was placed between two Philips XP2020Q detectors (coupled with BaF_2 scintillators) arranged co-linearly to ensure a high count rate. “Backscattering” effects [19,20] caused by the scintillator were suppressed by inserting a 7-mm thick lead plate between the sandwich and the detector of the start signal. The signal was processed by standard nuclear instrumentation modules and spectra were accumulated every 60 s and six data sets were then binned into one new data set to improve statistics. After subtracting the background and contributions from the source itself (salt, Kapton and positronium), the lifetime spectra were fitted using the program LT9 [21]. The spectrometer had a time resolution of ~ 0.250 ns and a count rate of ~ 600 s^{-1} , thus enabling data acquisition in a “fast mode” and an analysis with only one lifetime component τ_{IC} [11,22].

Hardness was measured using a MHT-10 microhardness tester. A load of 0.98 N was applied for 10 s. Each data point represents the average of 10 hardness measurements.

3. Results

3.1 Cu-containing alloys

3.1.1 PALS

Fig. 1a shows that the one-component positron lifetime τ_{IC} in various Al-Mg-Si alloys with and without Cu addition – alloys A2(Cu), A3(Cu) and A11(Cu) – evolves in a very similar manner as the previously investigated Al-Mg-Si alloys during NA [11]. Four typical PALS stages are observed:

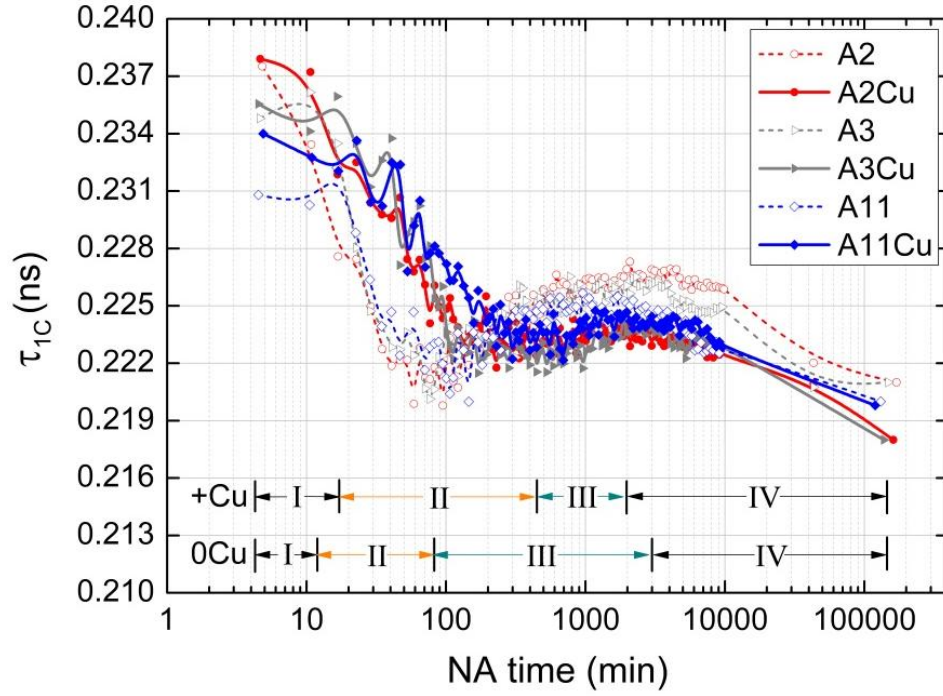
(I) Most alloys show a constant PLT (>0.230 ns) during the initial stage of NA (<20 min), indicated as “stage I” in Fig. 1a. For alloys with a low Mg content [11], e.g. alloy A2, such a stage is too short (<2 min) to be observed at “room temperature” due to the limited count rate of the spectrometer. In such alloys, the PLT has to be measured directly after quenching at sufficiently low temperatures (≤ 0 °C) in order to visualise this stage [18]. So far, the constant or slightly increasing PLT during stage I has not been explained.

(II) Until the end of stage II (local minimum of PLT), the PLT decreases monotonically to ~ 0.221 ns within $\sim 80 \pm 20$ min in Cu-free Al-Mg-Si alloys A2, A3 and A11, in a similar manner to the previously investigated alloys [11,18]. The analogous decrease of PLT to ~ 0.223 ns in the Cu-containing alloys A2Cu, A3Cu and A11Cu is about 5 times slower, i.e. ~ 500 min of NA is required to achieve the equivalent ageing state. The retarded clustering kinetics during stage II is illustrated by the orange arrows in Fig. 1a and black arrows in Fig. 1b.

(III) During subsequent stage III, a slight re-increase of PLT to ~ 0.224 ns is observed in Cu-containing alloys, while for Cu-free ones such a more pronounced increase to ~ 0.226 ns is found. The time to reach the local maximum of PLT is around 3000 min for Cu-free alloys, but just ~ 2000 min for the Cu-containing ones. Thus, Cu accelerates the ageing kinetics during stage III, see green arrows in Fig. 1a and black arrows in Fig. 1b. Note that the transition times reported here are longer than the ones reported in Ref. [11], possibly due to slightly different solute and impurity contents or natural ageing temperatures.

(IV) The PLT slowly re-decreases through the final stage IV to a value less than 0.221 ns after $\sim 10^5$ min of NA for all the alloys.

(a)



(b)

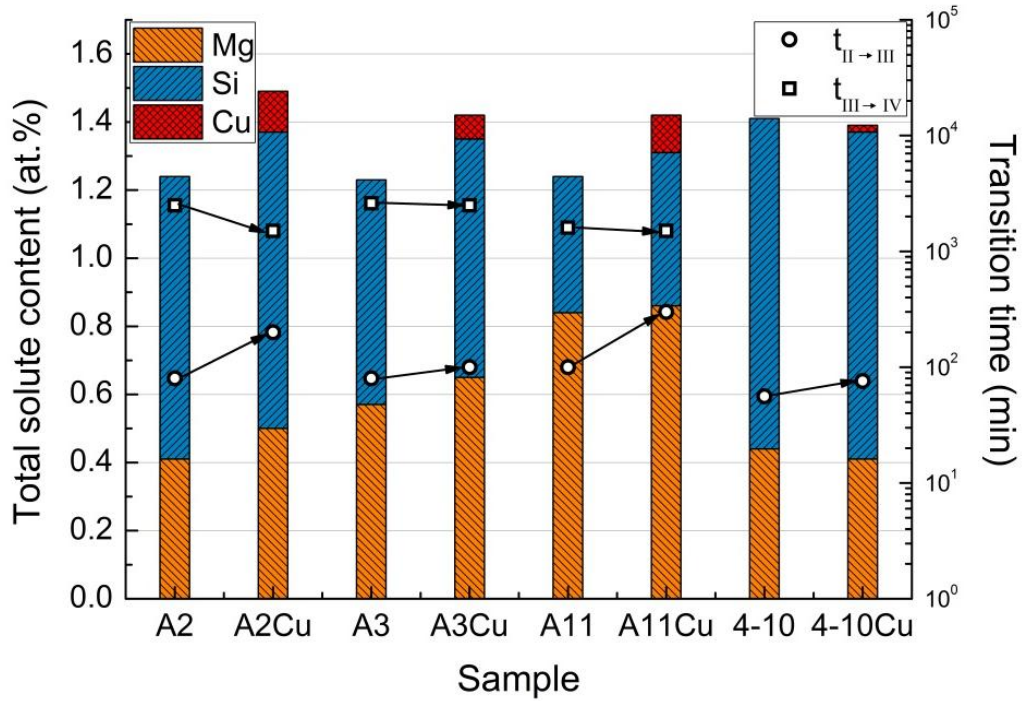


Fig. 1. (a) The one-component positron lifetime τ_{1C} as a function of NA time for various Al-Mg-Si and Al-Mg-Si-Cu alloys. The four stages observed during NA are marked I to IV. The NA kinetics of such alloys was measured in-situ. (b) Dependence of transition times $t_{II \rightarrow III}$ for stage II to III (black open spheres, right axis) and $t_{III \rightarrow IV}$ for stage III to IV (black open squares, right axis) on sample compositions (vertical bars, left axis).

Fig. 2 displays the PLT evolution in another set of samples, i.e. alloys 4-10 and 4-10Cu, to further substantiate the effect of Cu addition during RT storage. The Cu content is very low in alloy 4-10Cu – 0.02 at.%, i.e. 3-6 times lower than in the alloys discussed above – but the prolongation of stage II from ~60 min to 80 min due to the presence of Cu is clearly visible, see transition times t_{II-III} indicated by the blue and red arrows. This confirms the results shown in Fig. 1. For stage III, a similar evolution of PLT is observed for both alloys up to ~5000 min of NA and the end of stage III is hard to detect.

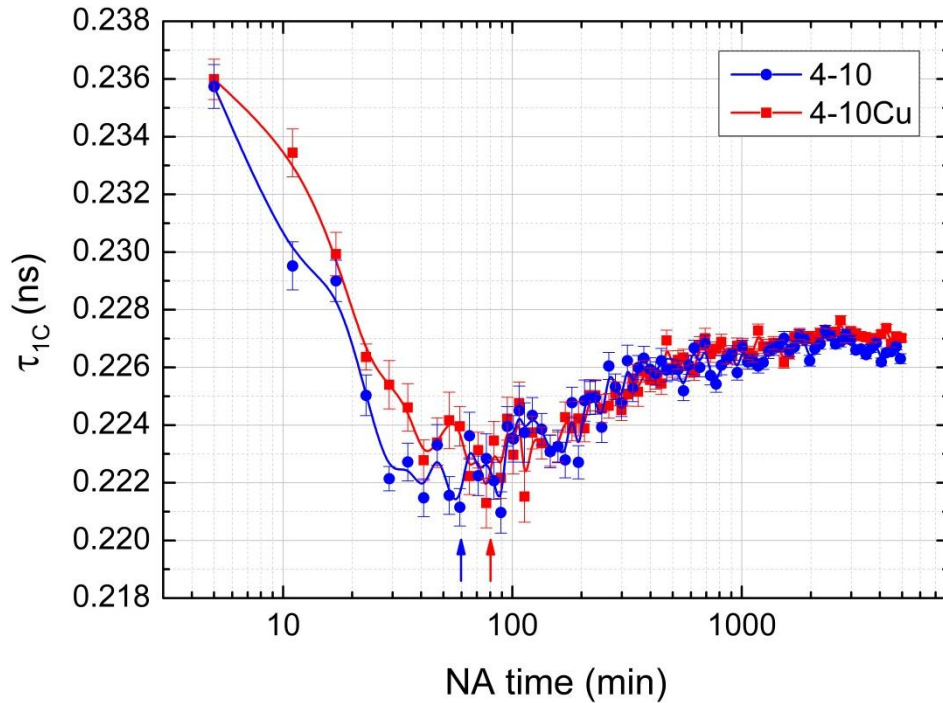


Fig. 2. As in Fig. 1a but for alloys 4-10 and 4-10Cu. Arrows point at lifetime minima.

3.1.2 Hardness

Fig. 3 shows the evolution of hardness of alloys 4-10 and 4-10Cu during NA, see red symbols. The hardness exhibits similar tendencies as the 1-component PLT shown in Fig. 1a, i.e. Cu retards (only slightly in this case due to the very limited Cu content) the formation of solutes clusters during the initial stage of NA (up to ~50 min), but promotes the growth of these clusters when NA proceeds, as indicated by the slower and faster increase of hardness of the Cu-containing alloy 4-10Cu, respectively. As a consequence of the two effects the data sets exhibit a crossover.

With higher Cu content, the retarded or accelerated increase of hardness with a crossover after ~ 1000 min or ~ 850 min can be more clearly observed in the commercial Cu-free 6022 (Al-0.68Mg-0.94Si) or Cu-added 6111 (Al-0.69Mg-0.95Si-0.31Cu) alloys, respectively [23] and also in the alloys A11 and A11Cu used in the current work [13], see blue symbols in Fig. 3. This feature also agrees with [24].

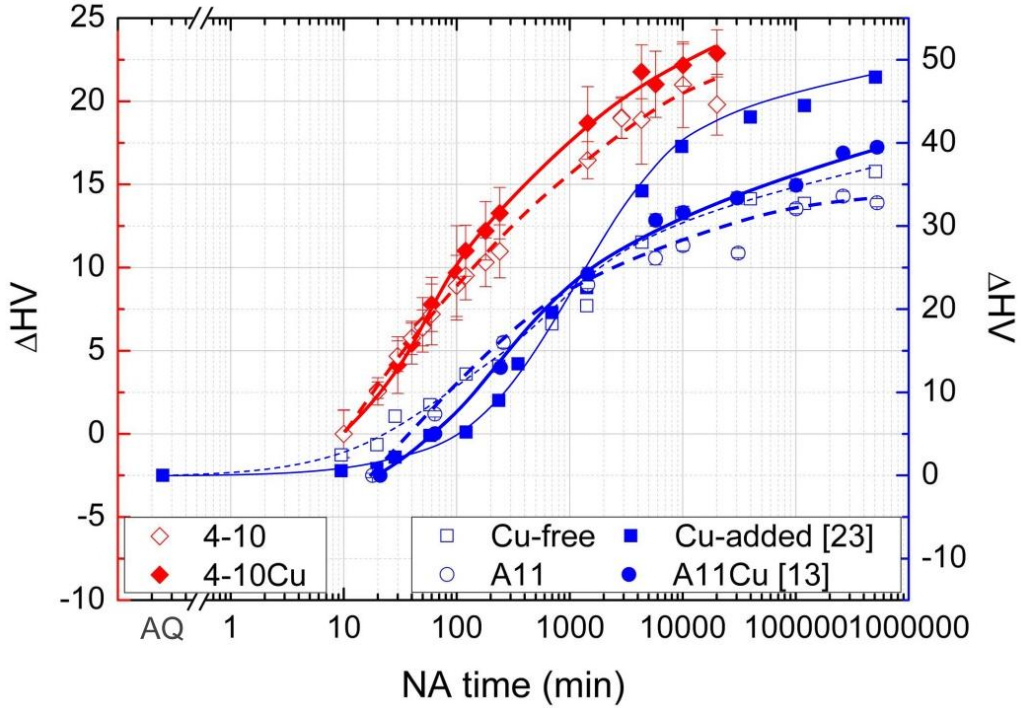


Fig. 3. Change of hardness during NA of Al-Mg-Si alloys with and without Cu addition. The measurements represented by circles and squares are from [13,23]. Lines are given to guide the eye. The as-quenched samples have been given a NA time less than 1 min.

3.2 Ge-containing alloys

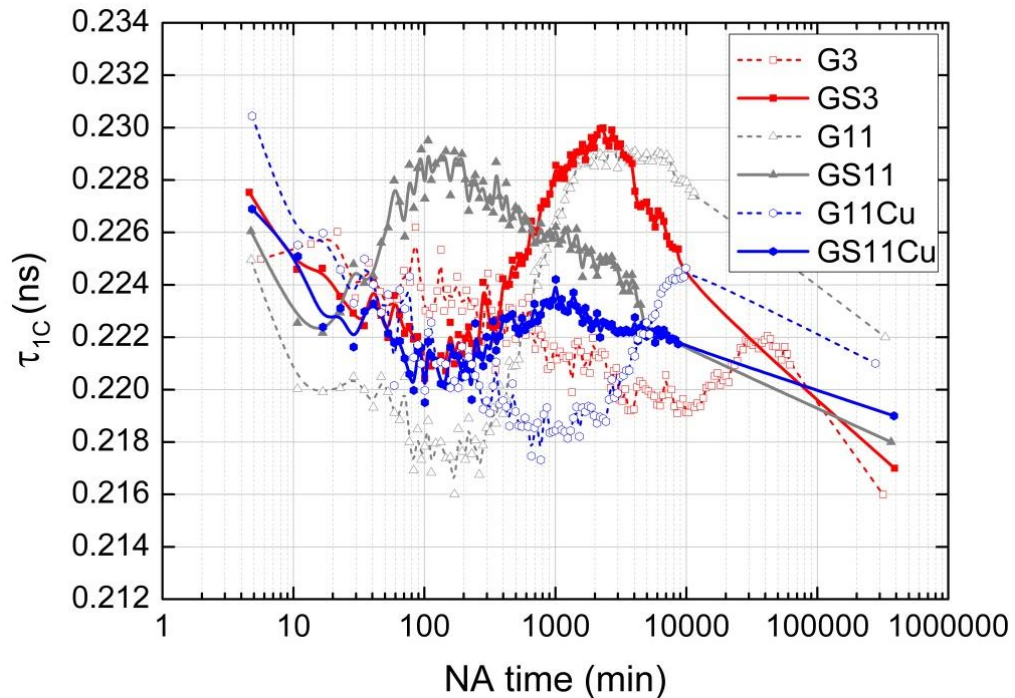
3.2.1 PALS

Fig. 4a shows a PLT evolution in Al-Mg-Ge and Al-Mg-Si-Ge(Cu) alloys during PALS stages II, III and IV (decrease, increase and re-decrease) similar to that described in Section 3.1.1, thus suggesting that Ge and Si interact with Mg in an analogous manner. Stage I cannot be observed for the Ge-containing alloys, except for one. Although both sets of alloys qualitatively show the same trend, the PLT evolution differs in two details concerning the amplitude of PLT variation (e.g. compare alloys G11 and G11Cu) as well as the transition times ($t_{II \rightarrow III}$ and $t_{III \rightarrow IV}$) between various PALS stages, both depending on the concentration of each alloying element. All the

transition times are given in Fig. 4b as a function of the solute concentration. By far the longest transition times $t_{II \rightarrow III}$ of ~ 10000 min and $t_{III \rightarrow IV}$ after ~ 41600 min of NA are observed in alloy G3 which contains the highest amount of Ge (0.59%). A much faster ageing kinetics is obtained in alloy G11 in which the Ge content is reduced to 0.14%, both transition times equal ~ 170 min and ~ 3500 min, respectively. With a $\sim 50\%$ higher Ge content but additional 0.31% Si it is found that the ageing kinetics of alloy GS3 is only slightly accelerated. The last sample, alloy GS11, which contains the highest Mg and some Si, but the lowest Ge content, shows the fastest ageing kinetics. Both transition times are markedly reduced to ~ 15 min and ~ 130 min.

A delayed clustering process during stage II is also observed in Al-Mg-Ge-Cu and Al-Mg-Si-Ge-Cu alloys with added copper, compare alloys G11 and G11Cu or GS11 and GS11Cu in Fig. 4a and b, respectively. Rather than the accelerated NA kinetics during subsequent ageing (stage III) as shown in Fig. 1a and b for Al-Mg-Si-Cu alloys, a further retardation of the NA kinetics during stage III is observed if Mg, Ge, Si and Cu co-exist in the alloy system.

(a)



(b)

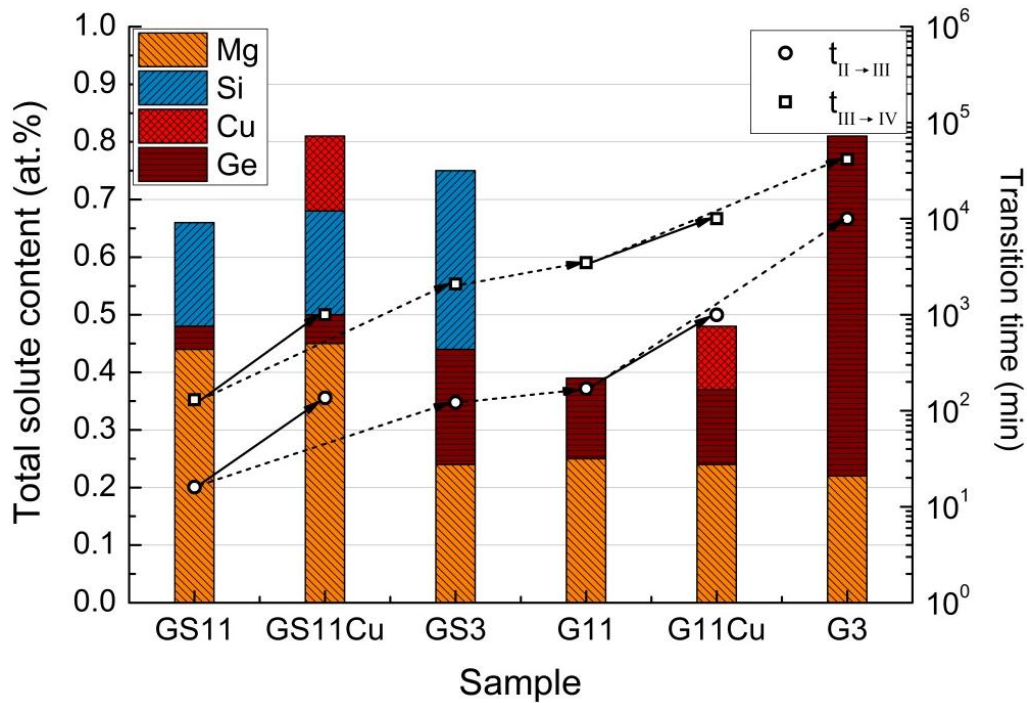


Fig. 4. As Fig. 1, but for alloys Al-Mg-Ge(Cu) and Al-Mg-Si-Ge(Cu).

3.2.2 Hardness

Fig. 5 shows the hardness evolution of the Ge-containing alloys during NA on both a logarithmic and a linear scale. All alloys investigated exhibit a similar hardness of ~ 35 HV after 10 min of NA. A rapid increase of hardness is observed during the first NA stage. This can be more clearly seen using the linear time scale in Fig. 5, see open symbols. In contrast, subsequent NA results in a much slower hardening response. After ~ 90000 min of NA, a hardness of ~ 65 HV is obtained for all the alloys.

Besides these common features, the fastest increase of hardness is observed for alloy GS11, which contains the highest amount of Mg and some Si but the lowest Ge content, while alloy G3 with the highest Ge content shows the slowest evolution of hardness, e.g. an comparable increase in hardness of 15 HV during the first 1000 min of NA of alloy GS11 is achieved by ageing alloy G3 for ~ 20000 min, see Fig. 5. The other two alloys lie in between. Thus, PALS reveals the same retarded NA kinetics of Ge-containing Al-Mg-Si alloys than hardness measurement.

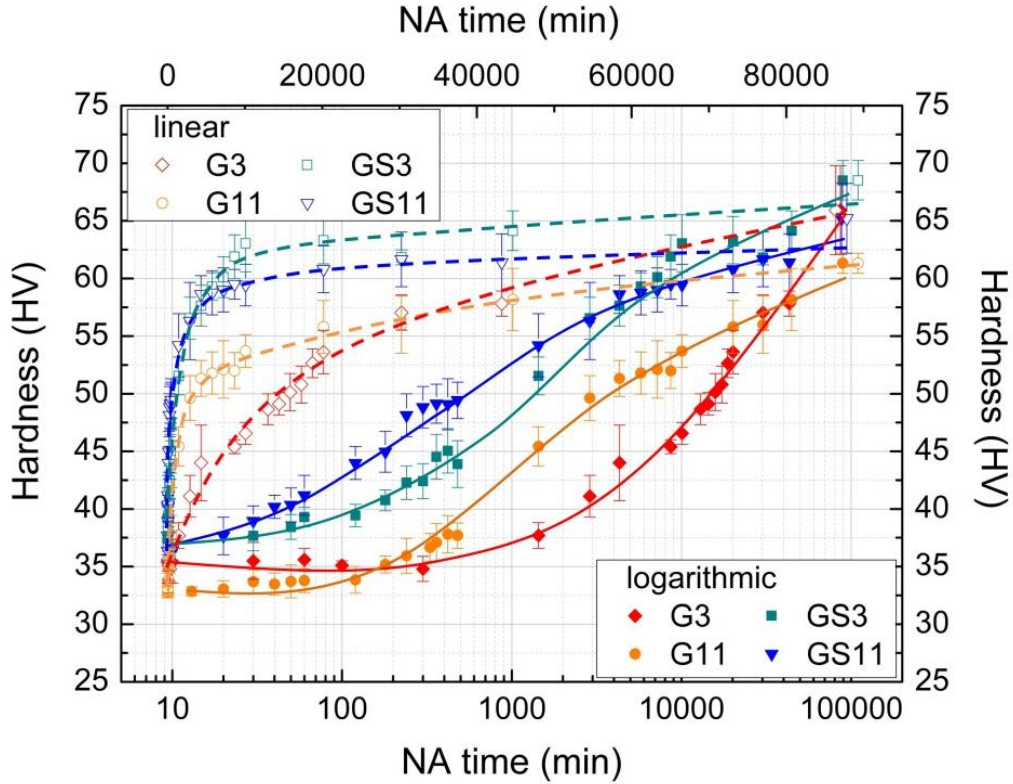


Fig. 5. Hardness evolution during NA in alloys G3, G11, GS3 and GS11. Each point represents the average of 10 hardness measurements. Solid and dashed lines are guide lines.

4. Discussion

4.1 General interpretation of PALS stages in Al-Mg-Si alloys

The observed evolution of PLT during NA in Fig. 1a is very similar to previous results [11]. Stage I is only visible if an alloy is aged at low temperatures ($\leq 0^\circ\text{C}$) [18], while for ageing at RT, high Mg and Si contents are required [11]. Formation, growth and coarsening (or ordering) of vacancy-free solute clusters were postulated as the general reason for the lifetime decrease, increase and re-decrease in stages II, III and IV, respectively. Particularly, by decomposing the lifetime spectra collected at low temperatures, the co-existence of 2 to 3 competing positron trapping mechanisms during the most complicated PALS stage II was experimentally verified [25,26]. On the one hand, vacancy-free solute clusters are rapidly formed during and after quenching and increasingly trap positrons (typical lifetime ~ 0.210 ns), while on the other the contribution from vacancy-solute complexes (~ 0.245 ns) gradually decreases. Thus, the combined effect of both leads to the typical decrease of τ_{IC} during stage II. During subsequent

stage III the increase of positron lifetime has been attributed to the incorporation of Mg into the previously formed Si-Mg clusters during which the Mg/Si ratio increases. This idea is supported by ^{25}Mg -NMR observations of an Al-0.46Mg-1.05Si-0.14Fe alloy [27]. The lower electron density caused by the large Mg atoms and the lower number of electrons then increases PLT [28,29]. In addition, it was found that stage III disappears if the Mg content is below 0.1% [18]. The emphasis of the discussion below is placed on stages II and III, while the final stage IV is not relevant in the context of this work.

4.2 Formation and growth of solute clusters

Because of the attractive interactions to the solute atoms in Al-Mg-Si alloys, see Fig. 6, vacancies created at the solutionising temperature (density $\sim 1.4 \times 10^{-4}$ /atom as calculated using the Lomer equation [30]) are largely preserved [18] immediately after quenching. A part will be gradually lost to vacancy sinks such as grain boundaries, dislocation loops, etc. The formation of vacancy clusters, which are formed in quenched pure Al, dilute Al-Mg and Al-Si alloys during NA [22], can be excluded in the case of Al-Mg-Si alloys due to the much higher probability of a vacancy to encounter a solute atom rather than another vacancy due to the high solute-to-vacancy ratio (~ 100). In the first place, quenched-in vacancies bind with a small fraction of the solutes and form mobile complexes. As NA proceeds, they assist the diffusion of certain solute atoms to other atoms and eventually form initial clusters. Because of the limited number of quenched-in vacancies the formation of new clusters or the further growth of existing ones will be possible only if vacancies are eventually released after spending some time at or in them to be able to transport more solute atoms. Under such circumstances, only a comparatively lower number of vacancy-containing solute clusters can be temporarily formed at a given time, the majority being vacancy-free.

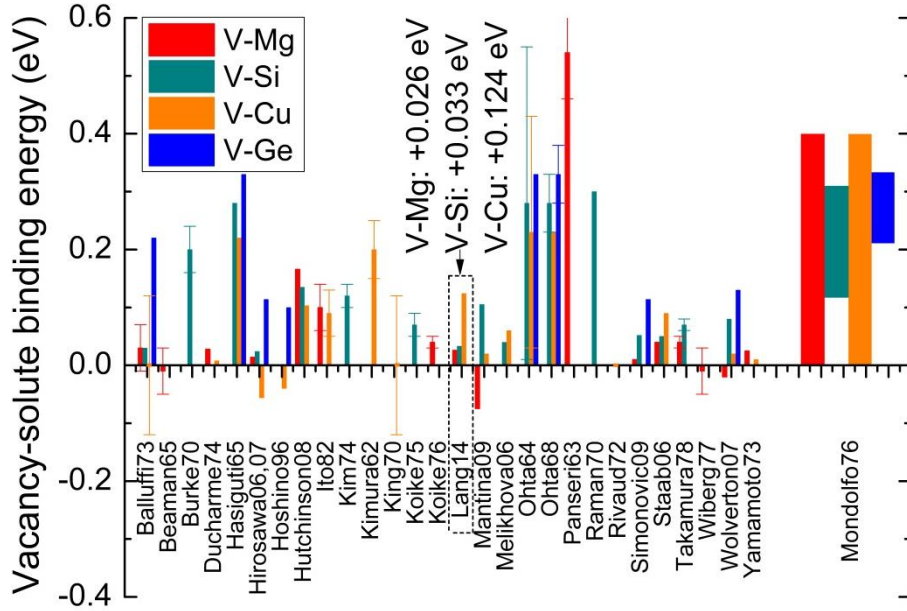


Fig. 6. Vacancy-solute binding energies from various sources (not all listed in References). Positive values refer to attractive binding, while negative ones denote repulsive interaction. Broad columns on the right hand side represent the range of binding energies between a vacancy and a certain solute atom, based on the collection of [31]. The data set [32,33] used for our interpretation is marked by a dashed box and the corresponding values are given.

During NA, solute clusters form and grow through the diffusion of solute atoms aided by vacancies, which are repeatedly trapped and de-trapped by and from these clusters. According to the total solute content (in the 1% range) of the alloys investigated in this study, each vacancy would have to deliver more than 100 atoms if all the solute atoms were used for clustering. As the size of the solute clusters increases, the release of vacancies becomes increasingly difficult, since the probability for a vacancy to escape from a cluster scales with $\exp(-ncE_b)$, with n the number of atoms in that cluster, c a constant and E_b the binding energy between a vacancy and a solute atom [34]. From this equation, one would expect a fast formation of solute clusters attributed to the high concentration of vacancies and solutes which are available for clustering during the initial stage of ageing, followed by an increasingly slower growth rate of these clusters due to the decreasing number of “free” vacancies as NA proceeds, since vacancies get either lost at sinks or are trapped increasingly longer by clusters. The presence of vacancy-solute complexes even after long NA in an Al-0.4Mg-0.4Si alloy was verified using temperature-dependent PALS [26]. This is plausible because otherwise the ageing process would quickly come to an end, whereas in reality it continues for at least 2 weeks [35].

4.3 Interaction energies between solutes and/or vacancies

In order to understand the phenomena caused by Cu and Ge, two-body interaction energies are important to know, since the formation of solute clusters and the rate at which vacancies detach from these clusters to transport more solutes strongly depends on the interaction energies between nearest neighbor solutes and/or vacancies in Al.

Based on first-principle calculations as given in Table 2, the interaction energies between Si-Si, Mg-Mg, Cu-Cu and Si-Cu in Al were found to be all negative (repulsive), while for Si-Mg and Mg-Cu, positive (attractive) interactions were estimated [36]. These interaction energies have been verified experimentally/theoretically, e.g. it was reported that the Mg/Si ratio in clusters increases due to the presence of Cu, pointing at the attractive interaction between Cu and Mg [12]. Such binding between solute atoms will be adopted for the following discussion.

Table 2. Various solute-solute [36] and vacancy-solute [32,33,37] interaction energies (in eV) taken from the literature to support our discussion. “+” sign refers to attractive binding.

Solute-solute	Si-Si	Mg-Mg	Cu-Cu	Si-Mg	Mg-Cu	Si-Cu
Interaction energy	-0.025	-0.037	-0.020	+0.042	+0.043	-0.038
Vacancy-solute	V-Si	V-Mg	V-Cu	V-Ge		
Interaction energy	+0.033	+0.026	+0.124	+0.053		

Many efforts have been made in the past to determine the binding energies between a vacancy and various kinds of solutes. A collection of such values are schematically summarized in Fig. 6. It is obvious that vacancies favor binding with the solute atoms relevant here according to most studies with a few exceptions, such as the weakly repulsive binding of V-Mg [37,38]. In order to enable the discussion, a quantitative comparison between various vacancy-solute binding energies is required. However, due to the different methodologies applied to determine such energies a comparison can hardly be made. Therefore, in this study, the interaction energy between a vacancy and a Cu atom is assumed to be attractive and stronger (at least comparable) than between a vacancy and either Si or Mg [31]. Furthermore, we adopt the values given in Table 2 that were calculated by first-principles [32,33]. We chose this set of values because it is the one where all three binding energies with Si, Mg and Cu have been determined on an equal footing with recent numerical methods. The pair V-Ge essentially shows a stronger binding than V-Si and V-Mg, as shown in Fig. 6. Thus, a value of +0.053 eV will be used, as suggested by [37], i.e. binding between V-Ge is 60% stronger than between V-Si.

4.4 Calculation of jump frequency

The jump frequencies f of vacancies attached to given solute atoms can be estimated using the following equation [39]:

$$f = f' \cdot \exp\left(-\frac{E_d - E_f - \Delta E_b}{k_B T}\right), \quad (1)$$

Where f' is the effective jump frequency (or vibrational frequency of an atom [40], based on the classical “five-frequency” model [41]). E_d is the diffusion activation energy of a vacancy, E_f is the vacancy formation energy (0.63 eV, the average of calculated LDA and GGA values from [38]), ΔE_b is the difference between the binding energies of a vacancy or solute atom with a nearest neighbor before and after the jump at the corresponding sites. To simplify the calculation, ΔE_b was neglected in this study. The values used by [39] were further adopted, based on [36,38,42], see Table 3. At “room temperature”, the calculated jump frequency of a vacancy associated with a Si atom in a Al matrix is equal to 18200 s^{-1} , while for V-Mg, a much lower value of 190 s^{-1} is obtained. The low mobility of a vacancy attached to a Mg atom at “room temperature” [43] has also been verified by measuring the average PLT in quenched Al-0.5%Mg and Al-1%Mg alloys NA for two months, during which only very small changes were observed [22]. For V-Cu, we obtain a value of 230 s^{-1} , similar to the one of V-Mg. Due to the unknown kinetic parameters for V-Ge, its corresponding jump frequency cannot be estimated.

Table 3. Kinetic parameters for the calculation of jump frequencies [38].

Kinetic parameters	Si	Mg	Cu
Attempt jump frequency f' (s^{-1})	1.57×10^{13}	1.86×10^{13}	1.09×10^{13}
Jump frequency f at 20 °C (s^{-1})	18200	190	230
Activation energy E_d (eV)	1.15	1.27	1.25

A direct correlation between the course of NA reflected by the time evolution of positron lifetimes and the jump frequency is not straightforward, since the precise determination of jump frequency depends on both activation energies E_d and ΔE_b in Eq. (1), which differ between various sources. Thus, the estimation of the jump frequencies merely serves as a qualitative explanation of the experimental observations.

4.5 Solute clustering in Cu-containing alloys

The formation and growth of solute clusters in Cu-free Al-Mg-Si alloys as described in [Section 4.2](#) will be notably affected by adding Cu. The interactions between vacancies and solute atoms (clusters) during PALS stages II and III are interpreted in the following.

4.5.1 Stage II (formation of solute clusters)

- **Formation of Cu-free clusters**

Once a vacancy is attached to a Si atom in Cu-free Al-Mg-Si alloys, it can move to other vacancies/solute atoms with a high jump frequency to form Si-Mg co-clusters [22], although V-Mg complexes diffuse only slowly. In the presence of Cu, a certain amount of quenched-in vacancies binds with Cu, forming V-Cu complexes beside V-Si and V-Mg. Due to the much higher binding energy V-Cu compared to V-Si and V-Mg the vacancies remain at the Cu sites for a much longer time than at Si or Mg sites. Due to the fact that the jump frequency of V-Cu is two orders of magnitude smaller than for Si, V-Cu complexes diffuse only slowly in the Al matrix. Under such circumstances, the migration of Si and Mg atoms and the rate of Si-Mg cluster formation is reduced to a certain extent as a result of Cu addition.

The interactions between V-Cu and Mg-Cu are both attractive, see [Fig. 6](#) and [Table 2](#). In contrast to the calculated repulsive interaction between Si and Cu given in [Table 2](#), [44] reported the existence of Si-Cu clusters besides Si-Mg and Si-Mg-Cu clusters using atom probe tomography, which manifests that the binding between Si and Cu is rather attractive. This implies that even if all vacancies bind with Si and Mg (due to their much higher abundance than Cu) and assist these atoms in forming only Cu-free Si-Mg clusters, the interactions between such complexes and Cu during diffusion cannot be ignored. As an example, due to the small distance between vacancy-related defects and solutes in the initial stage of NA, it is highly likely that on their way to emerging clusters, bare vacancies, V-Si or V-Mg complexes are temporarily trapped by Cu atoms if there are such in their vicinity. Indeed, this simple effect alone might be small due to the relatively low Cu content. However, as already mentioned in [Section 4.2](#), each vacancy has to transport Si and Mg atoms to form clusters repeatedly, which increases its chance to be trapped by a Cu atom.

- **Formation of Cu-containing clusters**

Not only Cu-free Si-Mg clusters but also considerable amounts of Cu-containing ones such as Si-Cu, Mg-Cu (containing on average 2–10 atoms) and Si-Mg-Cu (3–10 atoms) have been identified using atom probe tomography. It has been shown that after 2 h of NA, the number of clusters containing Cu is comparable to the number of binary Si-Mg clusters [44]. However, once Cu atoms are incorporated into the clusters, the clustering kinetics would be even slower. This is because vacancy de-trapping from Si-Mg-Cu clusters could be further retarded due to the stronger binding between V-Cu than between V-Si and V-Mg. The more Cu atoms are present in the clusters, the stronger the retardation effect might be. Moreover, V-Cu complexes diffuse only slowly towards clusters. As a result, smaller but more densely distributed clusters are formed at a given time due to Cu addition, since each vacancy can only transport few solutes to form clusters [45]. This coincides with the slightly higher positron lifetime between stages II and III for the Cu-containing alloys, see Fig. 1a, since it is cluster formation and growth that reduces positron lifetime during stage II. Quantitatively, the above proposition is supported by atom probe data [12], stating that the number density of clusters in Al-0.78Mg-0.68Si-0.30Cu alloy is 1.26 times higher than in Al-0.78Mg-0.68Si alloy after 1 week of NA (data for shorter NA time is not available). In another atom probe study, however, cluster number densities (containing at least 10 atoms) in Al-0.51Mg-0.94Si and Al-0.51Mg-0.95Si-0.34Cu alloys are almost identical after 1 week of NA [46]. The author noted that using only Mg and Si as cluster identifiers might account for the underestimation of the total cluster number density in Al-0.51Mg-0.95Si-0.34Cu alloy, in which a considerable amount of Cu-containing clusters are formed. In any case, it seems likely that adding Cu in an Al-Mg-Si alloy will lead to a higher number density of solute clusters during stage II.

Many authors observed a retarded clustering kinetics caused by Cu during NA. All these results coincide with our PALS observation. For example, [9] found a reduced rate of NA due to Cu addition in Al-Mg-Si alloys. Electrical resistivity measurements suggested a reduction of the migration rate of solute atoms by a factor of 10 due to the presence of Cu [47]. Using the same A11 and A11Cu alloys used in this work, [13] reported a monotonic increase of hardness for all alloys. The increase of hardness is lower in alloy A11Cu than in A11 during the first 850 min of NA, after which hardness increases to a higher value. The acceleration of clustering during PALS stage III by Cu will be explained in the next section.

4.5.2 Stage III (growth of solute clusters)

The smaller clusters formed in Cu-containing alloys during NA stage II are more densely distributed than in the Cu-free ones, in other words, the average distance d between clusters becomes shorter. When cluster growth set in during the subsequent NA stage III, the time t which is required for Mg atoms to migrate towards the pre-existing solute clusters is shortened to a certain extent. As an estimation, we assume a factor of 1.26 (as mentioned above) for the increase in cluster density n . Since the diffusion time t scales with x^2 , while the average cluster separation x scales with $n^{-1/3}$, the diffusion time is $t \sim n^{-2/3}$. Therefore, the migration time for a Mg atom to reach a cluster will be reduced to 0.86 the original value. Here, one should keep in mind that the determination of cluster number density and average cluster size by atom probe tomography can be affected by many factors such as detector efficiency or the cluster identification algorithm (mostly the maximum separation method). Still, the reduction in time agrees qualitatively with the observed shortening of stage III in Fig. 1 from ~3000 to ~2000 min.

The scenario proposed above that Cu retards the formation of clusters during stage II but stimulates their growth during stage III is consistent with the hardness evolution in A11/A11Cu [13], 4-10/4-10Cu and 6022/6111=6022Cu alloys as shown in Fig. 3. However, it has been also found that the hardness increase of A2Cu [13] and Al-0.4Mg-0.84Si-0.13Cu (at.%) alloys [48] (both are Si rich) are faster than the corresponding ones without Cu addition throughout NA, which is different from the observations shown in Fig. 1–3 for Mg rich Al-Mg-Si-Cu and Al-Mg-Si alloys, particularly the one on the right hand side of Fig. 3 which also deals with a Si-rich alloy. However, our observation of the Cu effect on clustering kinetics is further supported by a recent study [46], in which also Si-rich Al-Mg-Si(Cu) alloys were investigated. The idea that the varying effect of Cu on clustering correlates with the Mg/Si ratio of an alloy cannot be verified in this work.

4.6 Solute clustering in Ge-containing alloys

The effect of Ge addition on clustering cannot be discussed quantitatively in terms of atomic jump frequencies due to the lack of knowledge of the corresponding kinetic parameters. Nevertheless, it is likely that the diffusivity of a solute atom is affected by various factors such as atomic size, excess valence and solubility in Al [38]. Particularly, the atomic radius of Ge (1.25 Å) is larger than those of both Al (1.18 Å) and Si (1.11 Å). Thus, it appears plausible that

the diffusive movement of Ge atoms in the Al matrix is slow. With this assumption, the slowest ageing kinetics in Al-Mg-Ge alloy (G3) as shown in [Fig. 4](#) can be understood, since Mg (V-Mg) and Ge (V-Ge) atoms of both alloying elements migrate only slowly in Al. On the contrary, although the jump frequency of Mg (V-Mg) is low, the rate of clustering in Al-Mg-Si alloys is none the less much faster, benefiting from the rapid diffusion of Si (V-Si) towards Mg atoms. The much faster ageing kinetics of alloy GS3 than G3 further implies that at a given Mg content, Si facilitates cluster formation while Ge restrains it. Such an effect has been reported by many authors, for instance, the retarded NA kinetics in a Al-10Zn-0.12Ge alloy compared to an alloy containing an equal amount of Zn and 0.1% Si instead of Ge was clearly observed by measuring their electrical resistivity evolution at various temperatures (0 °C to 40 °C) after quenching [\[49\]](#). The compromised kinetics of clustering after partially substituting Si by Ge underlines the compensation effect between Si and Ge.

The idea mentioned above implies that if a vacancy has a larger binding energy with the additional solutes (e.g. Ge) than with Si and Mg atoms, the rate of clustering will be retarded due to a reduced number of vacancies available for assisting diffusion. This particularly applies to such systems where the added solutes do not interact with the main alloying elements. Although we cannot unambiguously determine the exact binding energy between a vacancy and a Ge atom, it has been proposed that there might be a correlation between the vacancy-solute binding energy and the size of a solute, i.e. strong binding occurs as a rule between a vacancy and a large solute atom (with possible exceptions such as Mg) [\[37\]](#). Therefore, a stronger binding between V-Ge than between V-Si as discussed in [Section 4.3](#) is very likely, owing to the larger atomic radius of Ge than of Si. Under such circumstances, in analogy to Cu-containing alloys, both effects together (low mobility of V-Ge complexes and reduced number of vacancies to deliver Si and Mg as a result of the stronger binding of V-Ge than of V-Si or V-Mg) would lead to the observed sluggish clustering kinetics in Ge-containing alloys.

5. Conclusions

The clustering kinetics in Cu and/or Ge-containing Al-Mg-Si alloys was investigated by applying positron annihilation lifetime spectroscopy and measuring hardness courses. The main findings are:

- The evolution of positron lifetime during NA follows qualitatively the same pattern for all the investigated alloys.
- Adding Cu to both Al-Mg-Si and Al-Mg-Ge alloys slows down the formation of solute clusters in an early stage. In Al-Mg-Si, Cu promotes their subsequent growth in a later stage.
- For alloys with equal Mg contents, Ge notably retards the ageing kinetics compared to Si. The alloy with the highest Mg and Si content shows the fastest NA kinetics, the alloy with the highest Ge content the slowest.
- All these effects can be explained by the vacancy-solute binding energies and the jump frequencies of vacancy-solute complexes.

In conclusion, the key to suppress the detrimental effect of NA on subsequent AA in industrial Al-Mg-Si alloys lies in controlling the vacancy-assisted diffusion of solute atoms. By adding a small amount of a proper alloying element such as Cu or Ge, the formation of solute clusters can be markedly retarded, provided that the binding between these additional solute atoms and vacancies is strong so that the number of available vacancies for solute diffusion is reduced and the corresponding jump frequencies are low. This finding is in accordance with the recent observation that a 40 ppm addition of Sn, which has a very strong binding to vacancies, can effectively retard NA for a very long time [50].

Acknowledgements

Funding from DFG (grant Ba 1170/22-1) and support from Prof. K. Maier (University Bonn), Prof. R. Krause-Rehberg (University Halle), C.D. Marioara (SINTEF), R. Holmestad (NTNU) and Dr. C.S.T. Chang (TU Berlin) are gratefully acknowledged.

References

- [1] M.L.V. Gayler, G.D. Preston, *J. I. Met.* 41 (1929) 191-247
- [2] I. Kovács, J. Lendvai, E. Nagy, *Acta Metall.* 20 (1972) 975-983.
- [3] H. Suzuki, M. Kanno, G. Itoh, *Aluminium* 57 (1981) 628-629.
- [4] L. Zhen, S.B. Kang, *Scripta Mater.* 36 (1997) 1089-1094.
- [5] R.S. Yassar, D.P. Field, H. Weiland, *Metall. Mater. Trans. A* 36A (2005) 2059-2065.
- [6] Y. Birol, *Scripta Mater.* 52 (2005) 169-173.
- [7] T. Masuda, Y. Takaki, T. Sakurai, S. Hirosawa, *Mater. Trans.* 51 (2010) 325-332.
- [8] Y. Yan, Z.Q. Liang, J. Banhart, *Mater. Sci. Forum* 794-796 (2014) 903-908.
- [9] D.W. Pashley, J.W. Rhodes, A. Sendorek, *Journal of the Institute of Metals London* 94 (1966) 41-49.
- [10] J. Banhart, C.S.T. Chang, Z.Q. Liang, N. Wanderka, M.D.H. Lay, A.J. Hill, *Adv. Eng. Mater.* 12 (2010) 559-571.
- [11] J. Banhart, M.D.H. Lay, C.S.T. Chang, A.J. Hill, *Phys. Rev. B* 83 (2011) 014101.
- [12] A.I. Morley, M.W. Zandbergen, A. Cerezo, G.D.W. Smith, *Mater. Sci. Forum* 519-521 (2006) 543-548.
- [13] S. Wenner, C.D. Marioara, S.J. Andersen, R. Holmestad, *Int. J. Mater. Res.* 103 (2012) 948-954.
- [14] K. Matsuda, J. Nakamura, K. Yamamoto, T. Kawabata, Y. Uetani, S. Ikeno, *Mater. Sci. Forum* 654-656 (2010) 930-933.
- [15] M. Liu, C.D. Marioara, R. Holmestad, J. Banhart, *Mater. Sci. Forum* 794-796 (2014) 971-976.
- [16] B. Lengeler, *Philos. Mag.* 34 (1976) 259-264.
- [17] R. Krause-Rehberg, H.S. Leipner, *Positron Annihilation in Semiconductors*, Springer, Heidelberg, 1999.
- [18] M. Liu, *Clustering kinetics in Al-Mg-Si alloys investigated by positron annihilation techniques*, (Ph.D. thesis), Technische Universität Berlin, 2014.
- [19] A. Dannefaer, *Appl. Phys. A* 26 (1981) 255-259.
- [20] L. Dorikens-Vanpraet, D. Segers, M. Dorikens, *Appl. Phys.* 23 (1980) 149-152.
- [21] J. Kansy, *Nucl. Instru. Meth. Phys. Res. A* 374 (1996) 235-244.
- [22] M. Liu, Y. Yan, Z.Q. Liang, C.S.T. Chang, J. Banhart, Influence of Mg and Si atoms on the cluster formation process in Al-Mg-Si alloys studied by positron annihilation lifetime spectroscopy, in: H. Weiland, A.D. Rollett, W.A. Cassada (Eds.), *Proceedings of the 13th International Conference on Aluminium Alloys (ICAA13)*, Pittsburgh, 2012, pp. 1131-1137.
- [23] J.H. Kim, T. Sato, *J. Nanosci. Nanotechnol.* 11 (2011) 1319-1322.
- [24] L.P. Ding, Z.H. Jia, Z.Q. Zhang, R.E. Sanders, Q. Liu, G. Yang, *Mater. Sci. Eng. A* 627 (2015) 119-126.
- [25] M. Liu, J. Čížek, C.S.T. Chang, J. Banhart, *Mater. Sci. Forum* 794-796 (2014) 33-38.
- [26] M. Liu, J. Čížek, C.S.T. Chang, J. Banhart, *Acta Mater.* 91 (2015) 355-364.
- [27] M.D.H. Lay, H.S. Zurob, C.R. Hutchinson, T.J. Bastow, A.J. Hill, *Metall. Mater. Trans. A* 43A (2012) 4507-4513.
- [28] M.J. Puska, R.M. Nieminen, *Rev. Mod. Phys.* 66 (1994) 841-897.
- [29] J.M. Campillo Robles, E. Ogando, F. Plazaola, *J. Phys. Condens. Matter* 19 (2007) 176222.

- [30] W.M. Lomer, *Vacancies and Other Point Defects in Metals and Alloys*, The Institute of Metals London, 1958.
- [31] L.F. Mondolfo, *Aluminium Alloys, Structure and Properties*, Butterworth, London, 1976.
- [32] P. Lang, Y.V. Shan, E. Kozeschnik, *Mater. Sci. Forum* 794-796 (2014) 963-970.
- [33] P. Lang, T. Weisz, M.R. Ahmadi, E. Povoden-Karadeniz, A. Falahati, E. Kozeschnik, *Adv. Mat. Res.* 922 (2014) 406-411.
- [34] H.S. Zurob, H. Seyedrezai, *Scripta Mater.* 61 (2009) 141-144.
- [35] C. Panseri, T. Federighi, *J. I. Met.* 94 (1966) 99-197.
- [36] S. Hirosawa, F. Nakamura, T. Sato, *Mater. Sci. Forum* 561-565 (2007) 283-286.
- [37] C. Wolverton, *Acta Mater.* 55 (2007) 5867-5872.
- [38] M. Mantina, Y. Wang, L.Q. Chen, Z.K. Liu, C. Wolverton, *Acta Mater.* 57 (2009) 4102-4108.
- [39] Z.Q. Liang, C.S.T. Chang, C. Abromeit, J. Banhart, J. Hirsch, *Int. J. Mater. Res.* 103 (2012) 980-986.
- [40] G.H. Vineyard, *J. Phys. Chem. Solids* 3 (1957)
- [41] J.B. Adams, S.M. Foiles, W.G. Wolfer, *J. Mater. Res.* 4 (1989) 102-112.
- [42] T. Hoshino, R. Zeller, P.H. Dederichs, *Phys. Rev. B* 53 (1996) 8971-8974.
- [43] G. Dlubek, O. Brummer, P. Hautojarvi, *Acta Metall.* 34 (1986) 661-667.
- [44] R.K.W. Marceau, A. de Vaucorbeil, G. Sha, S.P. Ringer, W.J. Poole, *Acta Mater.* 61 (2013) 7285-7303.
- [45] T. Federighi, G. Thomas, *Philos. Mag.* 7 (1961) 127-131.
- [46] M.W. Zandbergen, A. Cerezo, G.D.W. Smith, *Acta Mater.* 101 (2015) 149-158.
- [47] D.K. Chatterjee, K.M. Entwistle, *J. I. Met.* 101 (1973) 53-59.
- [48] M. Torsaeter, *Quantitative studies of clustering and precipitation in Al-Mg-Si(-Cu) alloys*, (Ph.D. thesis), Norwegian University of Science and Technology, 2011.
- [49] F. Hashimoto, M. Ohta, *J. Phys. Soc. Jpn.* 19 (1964) 1331-1336.
- [50] S. Pogatscher, H. Antrekowitsch, M. Werinos, F. Moszner, S.S.A. Gerstl, M.F. Francis, W.A. Curtin, J.F. Löffler, P.G. Uggowitzer, *Phys. Rev. Lett.* 112 (2014) 225701.